In Situ Growth of Cellular Two-Dimensional Silicon Oxide on Metal Substrates

Ferdaous Ben Romdhane,[†] Torbjörn Björkman,[‡] Julio A. Rodríguez-Manzo,[†,§] Ovidiu Cretu,[†,⊥] Arkady V. Krasheninnikov,[‡,∥] and Florian Banhart[†,*]

[†]Institut de Physique et Chimie des Matériaux, UMR 7504 CNRS, Université de Strasbourg, 23 Rue du Loess, 67034 Strasbourg, France, [‡]COMP/Department of Applied Physics, Aalto University, P.O. Box 11100, FI-00076 Aalto, Finland, [§]Department of Physics and Astronomy, University of Pennsylvania, Philadelphia, Pennsylvania 19104, United States, [⊥]Nanotube Research Center, National Institute of Advanced Industrial Science and Technology (AIST), Central 5, 1-1-1 Higashi, Tsukuba, Ibaraki 305-8565, Japan, and [∥]Department of Physics, University of Helsinki, P.O. Box 43, FI-00014 Helsinki, Finland

ABSTRACT Crystalline hexagonally ordered silicon oxide layers with a thickness of less than a nanometer are grown on transition metal surfaces in an *in situ* electron microscopy experiment. The nucleation and growth of silica bilayers and monolayers, which represent the thinnest possible ordered structures of silicon oxide, are monitored in real time. The emerging layers show structural defects reminiscent of those in graphene and can also be vitreous. First-principles calculations provide atomistic insight into the energetics of the growth process. The interplay between the gain in silica—metal interaction energy due to their epitaxial match and energy loss associated with the mechanical strain of the silica network is addressed. The results of calculations indicate that both ordered and vitreous mono/bilayer structures are possible, so that the actual morphology of the layer is defined by the kinetics of the growth process.

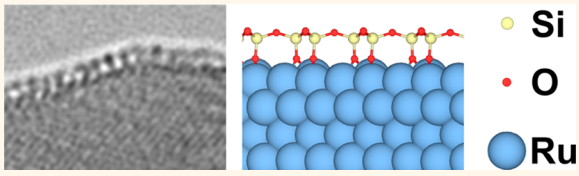

KEYWORDS: silica · two-dimensional crystals · electron microscopy · epitaxial growth

Layers of silicon oxide are important building blocks as insulating barriers in electronic devices, *e.g.*, as a gate oxide in field effect transistors. They are also used in catalysis for protecting metal surfaces. Thin layers of silicon oxide are normally amorphous without ordering above the scale of the molecular unit. On the other hand, the bulk phases of SiO_2 occur in several crystalline phases.

Recently, a considerable amount of attention has been paid to atomically thin silica films, and new quasi-two-dimensional phases of silica have been discovered.[1,2] The phases represent either a hexagonally ordered (crystalline) or disordered (vitreous) network of corner-sharing SiO_4 tetrahedra, forming a mono- or bilayer structure. The phases can be grown on various transition metals, such as Ru, Pt, Mo, Ni, Pd, and Cu,[2,3] and in the latter case the SiO_2 bilayer structure can even be isolated from the metal by etching the substrate. The attractive feature of these layers is their well-defined thickness of a monolayer or double layer. For applications in nanotechnology they could be more interesting than the commonly used amorphous silicon oxide films with varying thickness. Atomically thin silica films have also been grown between epitaxial graphene and Ru (0001) by stepwise intercalation of silicon and oxygen,[4] thus demonstrating the possibility of the electrical insulation of graphene without its transfer to an insulating substrate.

Although ordered and vitreous silica structures were already proposed as a two-dimensional glass by Zachariasen in 1932,[5] their thorough microscopic structural characterization was done only recently.[3,6,7] The cellular arrangement and the high flexibility of the network allow different bond angles, and so either a regular network of hexagons or a random arrangement of different polygons (*e.g.*, pentagons, hexagons, heptagons) appears.[7,8] The similarity to the structures of both perfect and defective graphene is striking,[9] with the honeycomb network of silica having almost twice the lateral dimensions as that

* Address correspondence to florian.banhart@ipcms.unistra.fr.

Received for review February 22, 2013 and accepted May 21, 2013.

Published online May 21, 2013
10.1021/nn400905k

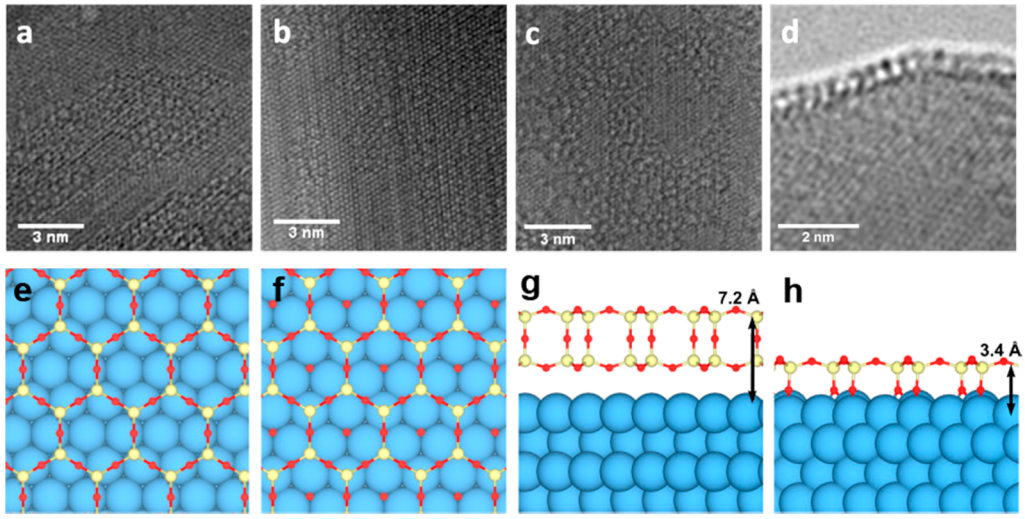

Figure 1. Ordered arrangement of SiO_2 cells in plan-view on (a) a Ru surface and (b) a Co surface, both grown at 440 °C. (c) Disordered structure with many nonhexagonal cells on a Fe surface grown at 470 °C. (d) Side-view of the cellular structure on Fe at 470 °C. The height of the cells is approximately 0.4 nm. Models of a SiO_2 structure on Ru as obtained from DFT calculations in top-view (e, f) and side-view (g, h). (e) and (g) show a double layer; (f) and (h) a monolayer structure. Si atoms are in yellow; O atoms in red.

of graphene. In this respect, the silica phase is a very interesting model system for studying structural defects and disorder in honeycomb lattices and their growth on metal substrates.

All studies so far reported an *ex situ* synthesis of the new silica phase and could not reveal details of the growth mechanism. Here, we report a new route toward the synthesis of 2D silica in a solid-state growth process that we have carried out *in situ* in a transmission electron microscope (TEM). Details of nucleation and growth are becoming accessible by direct observation, which sheds light on the growth mechanism. The epitaxial relationship between the silica layer and the metal as well as the crystalline symmetry of the metal surface are studied and combined with the results of density functional theory (DFT) calculations.

RESULTS

Different metals (Fe, Co, Ru) were deposited in separate experiments onto amorphous SiO_2 films by sputtering (see Methods section). Annealing at 700 °C for approximately 10 min in the heating stage of a TEM (pressure around 10^{-7} mbar) caused a transformation of the metal deposits, leading to crystalline metal platelets with a thickness of approximately 10 nm. A few minutes after cooling the specimen to 450 °C, the nucleation of a cellular structure started on the metal surface (Figure 1). The growth of this phase was observed to proceed during periods of several minutes. The structure appeared on Fe, Co, or Ru crystals at temperatures above 350 °C.

The cellular structure was visible in top-view on the metal layer as shown in Figure 1a–c. The contrast was weak but sufficient for observation when the metal layer had a thickness less than approximately 10 nm. In the side-view geometry, the layer appeared at the edge of the metal particles (Figure 1d), showing a cellular structure with a height above the metal substrate of approximately 0.3–0.4 nm. Areas with ordered hexagonal cells were observed on the (0001) surfaces of hexagonally close-packed Ru and Co layers (Figure 1a,b). The epitaxial match of the cellular arrangement with the metal lattice is apparent. For example, the silica hexagons are aligned along the $[10\bar{1}0]$ direction on the (0001) surfaces, and the size of a hexagon fits two lattice planes of the Ru or Co lattice (Figure 1a,b). On other metal surfaces, however, the cellular arrangements were rather disordered (Figure 1c). Generally, no long-range order of hexagonal cells appeared if the growth did not occur on the (0001) surfaces of hcp-Co or Ru. Models of the cellular SiO_2 structures as obtained from DFT calculations are shown in Figure 1e–h.

Typical nonhexagonal defects (pentagonal, heptagonal rings, *etc.*) appeared in all growth experiments (Figure 2). The defects in the honeycomb network are similar to those reported for graphene. Polygons from four- to nine-membered rings were observed (in some cases even larger rings appear). The morphologies of defects and amorphous areas are the same in ordered and in disordered networks and are similar to those reported previously.[7] Further examples are shown in the Supporting Information.

The nucleation of the silica cells started often at the intersection of planar defects with the metal surface. From there, the network was observed to spread over the metal until the growth was inhibited at surface steps or other defects. The growth dynamics is shown in a series of images and video 1 in the Supporting Information. Growth proceeds laterally with a speed on

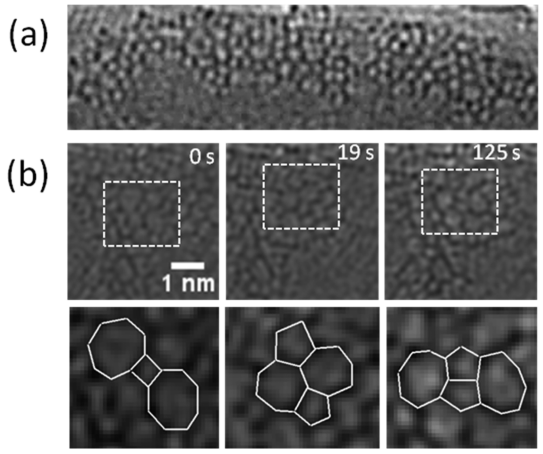

Figure 2. Structural defects in the hexagonal network in the structure grown at 470 °C on a Ru surface. (a) Arrangement of vertical defect lines (pentagon pairs, interrupted by heptagons or octagons) in a partially ordered network. (b) Evolution of a typical defect with time: two octagons, separated by a square (left), evolve into two pentagons and two heptagons (middle) and finally into two octagons, separated by two pentagons (right). The defects are highlighted with white lines in the enlarged sections (bottom row). The time between the recordings of the images is indicated.

the order of 0.4 nm/s at 450 °C. Experiments on Ru crystals that exhibited a large density of grains showed a preferential growth of the silica phase on the intersection of grain boundaries with the surface (see Section 6 of the Supporting Information). There, multilayer structures with larger and varying thickness appeared.

The structure is sensitive to the electron beam (200 keV) and disappears under intense irradiation. However, for the nucleation of the structure, a clean metal surface was necessary so that an intense "beam shower" was applied on a selected area of the metal prior to growth. Metal silicides were not observed as precursors of the silica phase, so we can exclude intermediate silicide phases.

The analysis of the samples by electron energy-loss spectroscopy (EELS) showed no elements other than the respective metal, silicon, and oxygen. The identification of SiO_2 by EELS was possible in both the side-view and plan-view geometry, but the signal from the thick metal substrate covers the Si and O edges in plan-view. When the focused electron beam was scanned across the surface of a metal particle covered with the silica layer, the Si edge appeared (Figure 3). The oxygen edge was too weak to be clearly identified; however, the Si edge shows the fine structure that is typical for SiO_2[10] and not for elemental silicon (see additional spectra in the Supporting Information).

In an attempt to get microscopic insights into the morphology of the silica layer and understand the nature of silica−metal bonding and the origin of defects, we carried out extensive DFT calculations (see the Methods section). The *bilayer* structure is

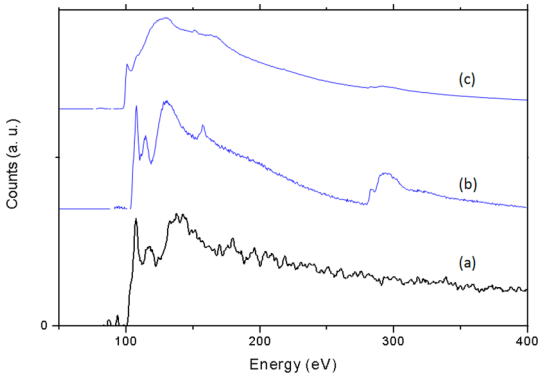

Figure 3. EELS identifying the cellular structure as SiO_2. (a) Experimental EEL spectrum of the structure on the edge of an iron particle (side-view orientation). (b) Reference EEL spectrum of SiO_2.[10] (c) Reference EEL spectrum of Si[10] (the reference spectrum (b) also shows a carbon K-edge at 280 eV that did not appear in the present experiments).

bound to the metal surface primarily by van der Waals (vdW) forces, and the binding energy was found to be −89 meV/(Si atom) = −14.0 meV/Å^2 for Ru and −62 meV/(Si atom) = −11.4 meV/Å^2 for Co, both in the typical range of binding energies of layered systems.[11] To estimate how important the relative position of the silica bilayer is with regard to the underlying metal atoms, we moved the bilayer periodically along the surface and found that the binding energy fluctuates by about 10 meV/(Si atom). By contrast, the bottom row oxygen atoms in the *monolayer* structure bind covalently to the surface, with a binding energy on the order of −3 eV/Si atom, and the maximum difference between different adsorption sites is 75 meV/(Si atom) for Ru and 210 meV/(Si atom) for Co. We also calculated both bilayer and monolayer structures on Ru with one additional oxygen atom per unit cell on the surface, as shown in Figure 1h. This is a stable configuration, also identified in the previous work by Löffler *et al.*,[6] but in contrast to the DFT calculations with a semilocal exchange/correlation functional augmented with an empirical vdW potential (PBE-D2 method),[12] which gave a decrease in the binding energy of about 30%, we see only very small differences in binding energy for both the bilayer (+3% binding energy) and monolayer configurations (difference <0.1%) when the oxygen is added. It has been shown that metals with strong adsorption of oxygen tend to form monolayers of silica, whereas weak oxygen adsorption (*e.g.*, noble metals) leads to bilayers of silica.[13] In view of the previously seen exaggeration of the dependence on atomic species of the PBE-D2 method for solids[14] as well as the insensitivity of the vdW binding to details of the chemistry in layered compounds,[11] the present result appears more likely, and we conclude that the presence of additional oxygen at the surface should not crucially affect the energetics of the electronic ground state in these systems.

To judge whether it may be energetically favorable for the silica system to distort, so as to be in registry with the underlying metal substrate, we also investigated the effect of straining the free-standing SiO_2 bilayer as well as the Si_2O_5 monolayer by calculating the total energy as a function of mechanical strain. For the free-standing monolayer system, we estimated the stress in the Si_2O_5 network bound to a metal surface by saturating the dangling oxygen bonds with hydrogen atoms. This emulates the effect of having a perfectly homogeneous metal surface that would allow the monolayer to assume its preferred shape.

The strain–energy curves for both systems are shown in Figure 4, and it is evident that the curves are very asymmetric, with the free-standing layers being much softer on the compression side. The reason for the difference in compressive and expansive strain, as illustrated in the insets of Figure 4, is that the oxygen tetrahedra of the undistorted lattice (right inset of Figure 4) can rotate to accommodate the strain (left inset of Figure 4), keeping the Si–O bond length fixed. When expanding the lattice, however, rotation of the tetrahedra is not possible, and the strain needs to be accommodated by elongation of the Si–O bonds, which costs much more energy.

Inspecting the energies involved in the binding of the *bilayer* silica to Co or Ru at the respective lattice constants of the metals, we see that the energy costs of deformation are of similar magnitude. However, the energy cost of sliding of a vdW bonded layer (10 meV/Si atom, as described above) is much lower

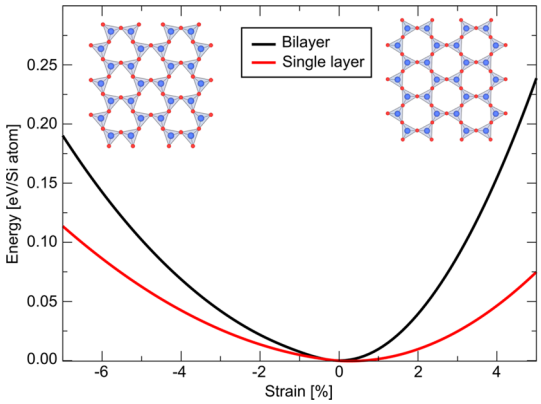

Figure 4. Energy as a function of strain for isolated bilayer and monolayer silica. The insets illustrate how the oxygen tetrahedra rotate to accommodate compressive strain, giving the asymmetric shape of the curves.

than the binding energy itself, so the pinning to the substrate is not strong enough to compress the lattice to the extent that we have done in these calculations. By contrast, for the covalently bonded *monolayer* structure the energy differences for different positions are much larger than the strain energy, and so the observed in-registry ordering of the silica on the substrate again confirms the monolayer as the observed structure.

The calculated data are summarized in Table 1. To estimate the stability of the two structures on the surfaces, we calculated a bilayer figure of merit, which represents a gain/loss in energy of a bilayer with respect to the monolayer structure, as shown schematically in the Supporting Information. Additional oxygen atoms were added to the metal surface to make the number of Si and O atoms the same in both cases. The figure of merit (E_{merit}) can then be expressed as

$$E_{merit} = E(SiO_2@M) + 2E(O@M) - [2E(Si_2O_5@M) + E(M)]$$

where $E(SiO_2@M)$ is the total energy of the bilayer on a metal slab, $E(O@M)$ is the total energy of the metal slab with O adatom, $E(Si_2O_5@M)$ is the total energy of the monolayer on a metal slab, and $E(M)$ is the total energy of the slab. This corresponds to oxygen-rich conditions with infinite availability of the metal surface. The conclusion is that the bilayer is more stable on the Ru surface, while the monolayer should be preferable on Co. We stress however that the energy difference is quite small, and the actual structure to be grown may be governed by the kinetics of the process.

We further studied the energetics of a free-standing silica bilayer when 5577 and similar defects are introduced. In agreement with previous results,[7] we found that it costs relatively little energy to create nonhexagonal rings: the formation energy of an isolated 5577 defect is 3.7 eV. When the separation between the defects is small and the supercell shape/size is optimized, this value decreases drastically, demonstrating that the formation of a random network by means of rotating bonds in the hexagonal structure is expected to be easy.

Nevertheless, the loss in energy when defects are formed is larger than the gain in vdW energy due to a better registry between the metal and substrate atoms. Thus, the formation of nonhexagonal rings (which are out of equilibrium) is rather due to the details of the growth process than substrate–metal interaction.

TABLE 1. Energetics of Mono- and Bilayer Silica Structures on Metals[a]

TM	struct.	*a* (Å)	mismatch	SL strain energy	BL strain energy	SL binding energy	BL binding energy	O heat of dissociative adsorption	bilayer figure of merit
Ru	hcp	5.411	+1.9%	0.008 eV/Si	0.036 eV/Si	−3.602 eV/Si	−0.089 eV/Si	−2.9 eV/O	−0.168 eV/SiO_2
Co	hcp	5.014	−5.6%	0.076 eV/Si	0.126 eV/Si	−3.571 eV/Si	−0.062 eV/Si	−2.7 eV/O	+0.129 eV/SiO_2

[a] A negative value of the figure of merit indicates that the bilayer structure is energetically preferable over the monolayer. The energy difference is relatively small for both Ru and Co.

However, for monolayers, where the substrate−silica interaction is much stronger, the effects of metal substrate should play a considerable role, so that surface defects and atomic steps may facilitate formation of the vitreous structures.

DISCUSSION

The structure of the 2D silica cells that was observed in the top-view orientation in this study is in accordance with previous observations (ref 2 and references therein). The similarity with the catalytic growth of carbon nanotubes[15] or graphene[16] on a metal substrate in a solid-state growth process is apparent. The measured height of the layer in side-view images (0.3−0.4 nm) corresponds to the thickness of a silica monolayer rather than to a bilayer structure. This is also supported by simulations of the electron microscopy images of both structures (see Supporting Information), where the double-layer structure shows two fringes above the metal surface, which is not observed experimentally. The cellular structure was always stationary, indicating strong bonding between the metal and the layer. This is predicted for a monolayer (Figure 1) but not for a double layer, where only weak van der Waals bonding between the layer and the substrate is expected.[2] In the latter case, one would expect a certain lateral mobility of the layer.

The nucleation and growth is a pure solid-state mechanism that can be explained either by bulk or by surface diffusion of silicon and oxygen atoms through/on the metal layers. The scenario of bulk diffusion is supported by the observation of preferential nucleation on grain boundaries, where the diffusion of Si atoms should be facilitated (see Section 6 of the Supporting Information). Our DFT simulations of Si interstitial diffusion in bulk Co and Ru give migration barriers of 1.2 and 0.8 eV, respectively, indicating that Si atoms should be mobile at the experimental temperatures. Since the interstitial formation enthalpy is high (2.5 and 4.3 eV for Co/Ru), the solubility of Si in the metals should be very low. However, since the process occurs far from thermal equilibrium, the migration of Si and O atoms might rather be governed by kinetics than by energetics of foreign atoms in the metal particles.

The oxygen could originate either from the SiO_2 substrate or from a native metal oxide film on the metal particles (such a film was not visible in the TEM images, however). As soon as the Si (and O) atoms reach the metal surface, where an extremely thin metal oxide layer might be present, the Si reduces the metal and oxidizes by forming the cellular phase. In this case, diffusion of oxygen through the metal would not be necessary, but independent oxygen diffusion, leading to the reaction with Si atoms at the metal surface, can be imagined as well. The alternative scenario would be the independent surface diffusion of Si and O atoms on the metal particles (that are small in this experiment) until they reach pinning sites where the nucleation of a silica cell starts. This has already been studied in the context of the role of Si and O diffusion in the growth of metals on oxide-covered Si substrates.[17,18]

After the nucleation of one cell, the growth proceeds laterally on the metal surface. Surface steps or intersections of planar defects with the metal surface act as nucleation sites but could also hinder the lateral propagation of the layer. This might be the reason that coherently ordered growth is always limited laterally. Since the cellular structure is highly flexible under lateral stress (*cf.* Figure 4 and Table 1), a moderate mismatch with the substrate should not limit lateral growth of silica, and we can assume that, in an optimized experiment, the size of the metal islands themselves limits the lateral extension of the silica phase. On a flat metal film with a low density of surface defects (steps, *etc.*), extended silica layers could be grown that are large enough for possible applications.

CONCLUSIONS

Mono- and bilayers of ordered and disordered silica were grown on transition metal surfaces. *In situ* electron microscopy allowed us to monitor the nucleation and growth in real time and at atomic resolution. Structural defects were observed that have the same geometry as reconstructed vacancies in graphene layers. As a condition for an ordered arrangement of the hexagonal cells, an epitaxial match with a metal surface of hexagonal symmetry was found. The growth of silica on metal substrates is an important technique to produce extremely thin oxide films of a well-defined thickness. The present study shows the dynamics of growth and indicates that monolayer films are favorable energetically with respect to bilayers under certain conditions. The monolayers constitute the thinnest possible silicon oxide films. It can be expected that these oxide films find applications as insulating layers in nanoelectronic devices or as tunneling barriers.

METHODS

A. Experimental Section. Amorphous SiO grids that are available commercially as TEM specimen supports were annealed in air at 350 °C and thus oxidized to films of SiO_2 that had an initial thickness on the order of 10 nm. Different metals (Fe, Co, Ru) were deposited in separate experiments on the SiO_2 films by sputtering. The grids were then transferred to a heating stage in a TEM (Jeol 2100F with C_s-corrected condenser, operated at 200 kV). Annealing at 700 °C in the microscope caused a transformation of the deposited metal films, leading either to

isolated crystalline platelets with a thickness of approximately 10 nm in the case of Fe or Co or, in the case of Ru, to a partially coherent film of nanocrystallites with a high density of grain boundaries. After cooling to 450 °C, the metal layers on the SiO_2 film were exposed for a few minutes to an intense electron beam that resulted in a cleaning of the metal surface, so that no residues of amorphous SiO_2 were left.

B. Calculations. We used the plane-wave-basis-set Vienna ab initio simulation package.[19,20] Projector augmented wave potentials[21] were employed to describe the core electrons. To account for the weak van der Waals forces previously found to be decisive in the substrate binding for the bilayer structure,[3,6] we use the nonlocal vdW density functional PW86R-VV10sol.[22] The calculations were performed with a primitive SiO_2 cell stretched or contracted to match the surface 2×2 supercell of hcp Co or Ru. The Brillouin zone was sampled by a 7×7 mesh, corresponding to a grid spacing of approximately 0.2 $Å^{-1}$, which was found sufficient to faithfully represent bulk properties of the metal such as a Co magnetic moment of $\sim$1.7 μ_B. The surface was modeled as a four-layer slab with fixed bottom layer and a vacuum of 16 Å separating the repeating images.

Conflict of Interest: The authors declare no competing financial interest.

Acknowledgment. Support by the French Agence Nationale de Recherche (project NANOCELLS, ANR12 BS1000401) and Academy of Finland (projects 218545 and 263416) is gratefully acknowledged. We further thank CSC Finland and the Aalto Science-IT project for generous grants of computer time. The authors also thank C. Pham-Huu for valuable discussions and M. Acosta for technical assistance in the sputtering experiments.

Supporting Information Available: Simulated electron microscopy images are shown in comparison with the experimental images to confirm the structure model. Further electron microscopy images show the nucleation and growth of the structure. Electron energy-loss spectra, images from structural defects, and the growth of the silica phase on grain boundaries are shown. Finally, details about the calculation of the figure of merit are given. A video shows the growth of a silica layer on a Co substrate. This material is available free of charge *via* the Internet at http://pubs.acs.org.

REFERENCES AND NOTES

1. Weissenrieder, J.; Kaya, S.; Lu, J.-L.; Gao, H.-J.; Shaikhutdinov, S.; Freund, H.-J.; Sierka, M.; Todorova, T. K.; Sauer, J. Atomic Structure of a Thin Silica Film on a Mo(112) Substrate: A Two-Dimensional Network of SiO_4 Tetrahedra. *Phys. Rev. Lett.* **2005**, *95*, 076103.
2. Shaikhutdinov, S.; Freund, H.-J. Ultrathin Silica Films on Metals: The Long and Winding Road to Understanding the Atomic Structure. *Adv. Mater.* **2013**, *25*, 49–67.
3. Huang, P. Y.; Kurasch, S.; Srivastava, A.; Skakalova, V.; Kotakoski, J.; Krasheninnikov, A. V.; Hovden, R.; Mao, Q.; Meyer, J. C.; Smet, U.; *et al*. Direct Imaging of a Two-Dimensional Silica Glass on Graphene. *Nano Lett.* **2012**, *12*, 1081–1086.
4. Lizzit, S.; Larciprete, R.; Lacovig, P.; Dalmiglio, M.; Orlando, F.; Baraldi, A.; Gammelgaard, L.; Barreto, L.; Bianchi, M.; Perkins; *et al*. Transfer-Free Electrical Insulation of Epitaxial Graphene from its Metal Substrate. *Nano Lett.* **2012**, *12*, 4503–4507.
5. Zachariasen, W. H. The Atomic Arrangement in Glass. *J. Am. Chem. Soc.* **1932**, *54*, 3841–3851.
6. Löffler, D.; Uhlrich, J. J.; Baron, M.; Yang, B.; Yu, X.; Lichtenstein, L.; Heinke, L.; Büchner, C.; Heyde, M.; Shaikhutdinov; *et al*. Growth and Structure of Crystalline Silica Sheet on Ru(0001). *Phys. Rev. Lett.* **2010**, *105*, 146104.
7. Lichtenstein, L.; Büchner, C.; Yang, B.; Shaikhutdinov, S.; Heyde, M.; Sierka, M.; Włodarczyk, R.; Sauer, J.; Freund, H.-J. The Atomic Structure of a Metal-Supported Vitreous Thin Silica Film. *Angew. Chem., Int. Ed.* **2012**, *51*, 404–407.
8. Wlodarczyk, R.; Sierka, M.; Sauer, J.; Löffler, D.; Uhlrich, J. J.; Yu, X.; Yang, B.; Groot, I. M. N.; Shaikhutdinov, S.; Freund, H.-J. Tuning the Electronic Structure of Ultrathin Crystalline Silica Films on Ru(0001). *Phys. Rev. B* **2012**, *85*, 085403.
9. Banhart, F.; Kotakoski, J.; Krasheninnikov, A. V. Structural Defects in Graphene. *ACS Nano* **2011**, *5*, 26–41.
10. Ahn, C. C.; Krivanek, O. L. *EELS Atlas*; ASU HREM Facility and Gatan Inc., 1983.
11. Björkman, T.; Gulans, A.; Krasheninnikov, A. V.; Nieminen, R. M. van der Waals Bonding in Layered Compounds from Advanced Density-Functional First-Principles Calculations. *Phys. Rev. Lett.* **2012**, *108*, 235502.
12. Grimme, S. Semiempirical GGA-Type Density Functional Constructed with a Long-Range Dispersion Correction. *J. Comput. Chem.* **2006**, *27*, 1787–1799.
13. Yu, X.; Yang, B.; Boscoboinik, J. A.; Shaikhutdinov, S.; Freund, H.-J. Support Effects on the Atomic Structure of Ultrathin Silicon Films on Metals. *Appl. Phys. Lett.* **2012**, *100*, 151608.
14. Björkman, T.; Gulans, A.; Krasheninnikov, A. V.; Nieminen, R. M. Are We van der Waals Ready? *J. Phys.: Condens. Matter* **2012**, *24*, 424218.
15. Rodriguez-Manzo, J. A.; Janowska, I. M.; Pham-Huu, C.; Tolvanen, A.; Krasheninnikov, A. V.; Nordlund, K. H.; Banhart, F. Growth of Single-Wall Carbon Nanotubes from Sharp Metal Tips. *Small* **2009**, *5*, 2710–2715.
16. Rodriguez-Manzo, J. A.; Pham-Huu, C.; Banhart, F. Graphene Growth by a Metal-Catalyzed Solid-State Transformation of Amorphous Carbon. *ACS Nano* **2011**, *5*, 1529–1534.
17. Barski, A.; Derivaz, M.; Rouvière, J. L.; Buttert, D. Epitaxial Growth of Germanium Dots on Si(001) Surface Covered by a Very Thin Silicon Oxide Layer. *Appl. Phys. Lett.* **2000**, *77*, 3541.
18. Hur, T.-B.; Kim, H. K.; Blachere, J. Epitaxial Growth of Ag Films on Native-Oxide-Covered Si Substrates. *Phys. Rev. B* **2007**, *75*, 205306.
19. Kresse, G.; Furthmüller, J. Efficient Iterative Schemes for *ab Initio* Total-Energy Calculations Using a Plane-Wave Basis Set. *Phys. Rev. B* **1996**, *54*, 11169–11186.
20. Kresse, G.; Furthmüller, J. Efficiency of ab-Initio Total Energy Calculations for Metals and Semiconductors Using a Plane-Wave Basis Set. *Comput. Mater. Sci.* **1996**, *6*, 15–50.
21. Blöchl, P. E. Projector Augmented-Wave Method. *Phys. Rev. B* **1994**, *50*, 17953–17979.
22. Björkman, T. van der Waals Density Functional for Solids. *Phys. Rev. B* **2012**, *86*, 165109.